Electronic Supplementary Information

Turning Berlin Green Frameworks into Cubic Crystals for Cathodes with High-Rate Capability

Jeong Yeon Heo,[‡a,b] Ju-Hyeon Lee,[‡a,b] Jin-Gyu Bae,[a,b] Min Sung Kim,[a,b] Hyeon Jeong Lee*[c] and Ji Hoon Lee*[a,b]

[a] School of Materials Science and Engineering, Kyungpook National University, Daegu, 41566, Republic of Korea

[b] KNU Advanced Material Research Institute, Kyungpook National University, Daegu, 41566, Republic of Korea

[c] Department of Materials Science and Engineering, Ulsan National Institute of Science and Technology, Ulsan 44919, Republic of Korea

‡: These authors contribute equally.

*Corresponding authors:

H. J. Lee (hyeonjeong.lee@unist.ac.kr), J. H. Lee (jihoonlee@knu.ac.kr)

Keywords: Crystal engineering, Morphological transition, Prussian blue analogues, Metal–ligand interaction, X-ray diffraction

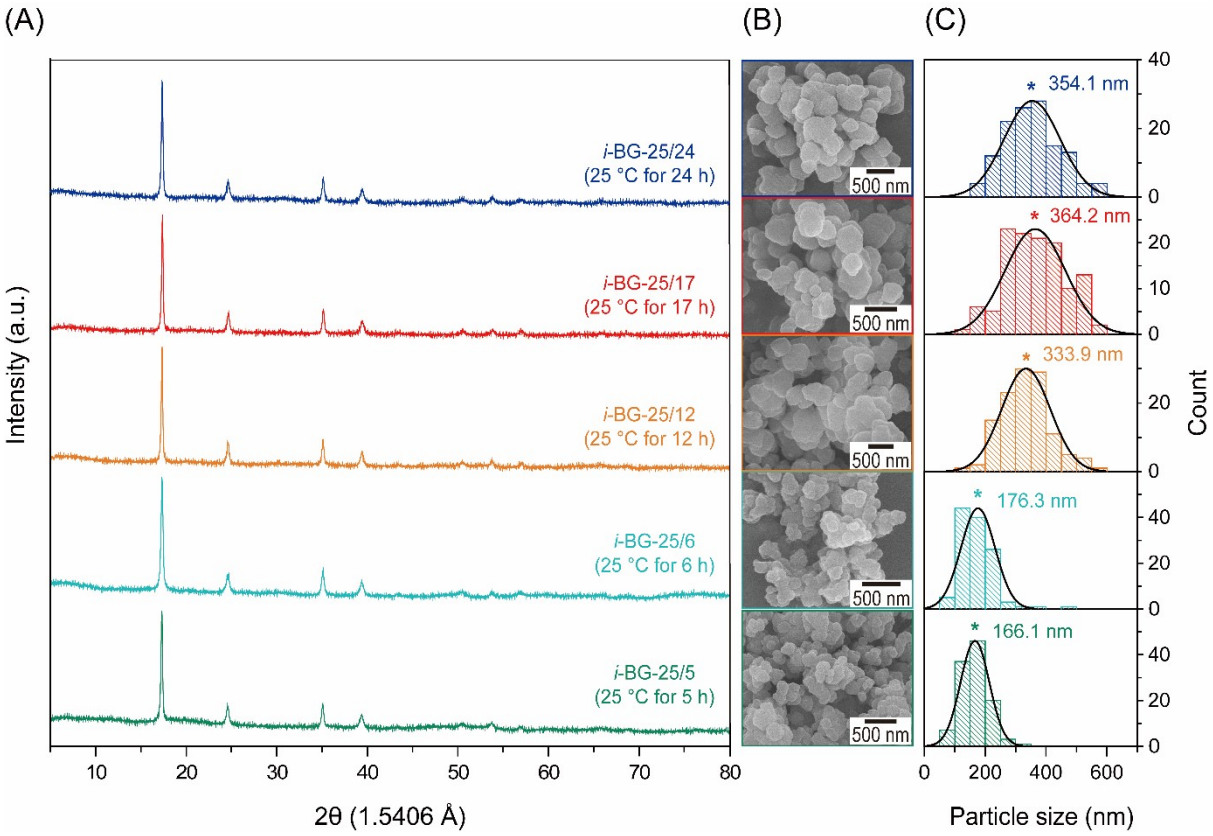

Fig. S1. (A) XRD patterns and (B) SEM images of a series of *i*-BG-25/t samples. (C) Particle size distribution curves of *i*-BG-25/t samples.

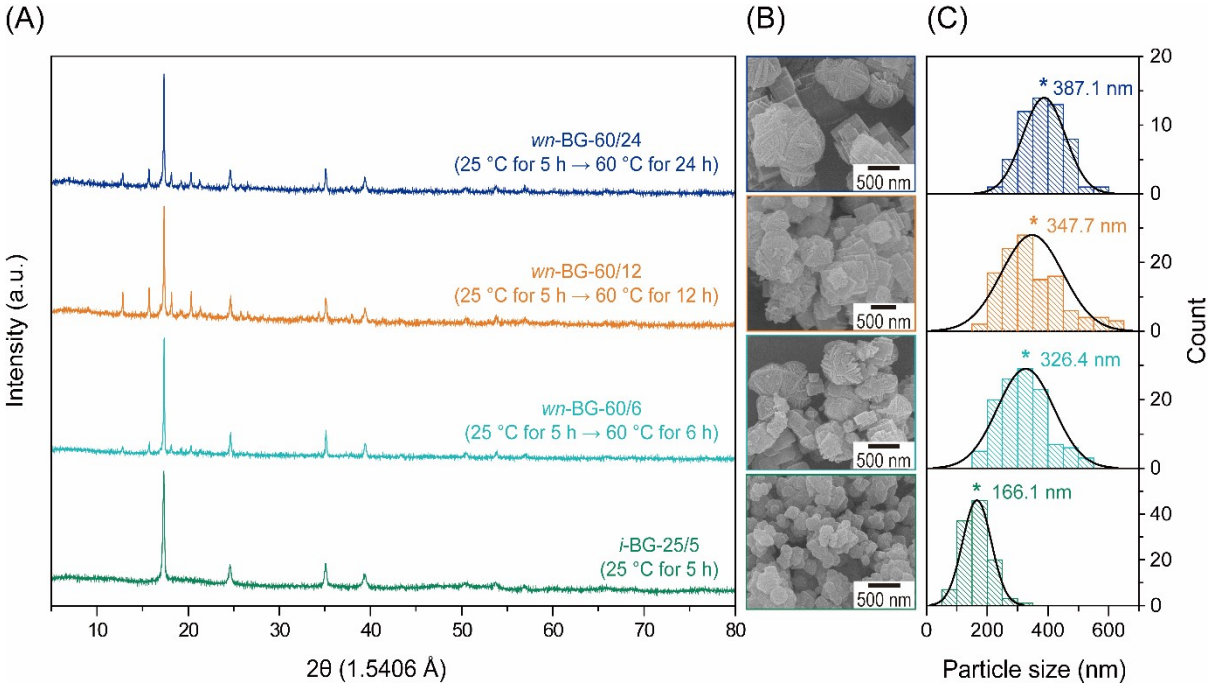

Fig. S2. (A) XRD patterns and (B) SEM images of a series of *wn*-BG-60/t samples. (C) Particle size distribution curves of *wn*-BG-60/t samples.

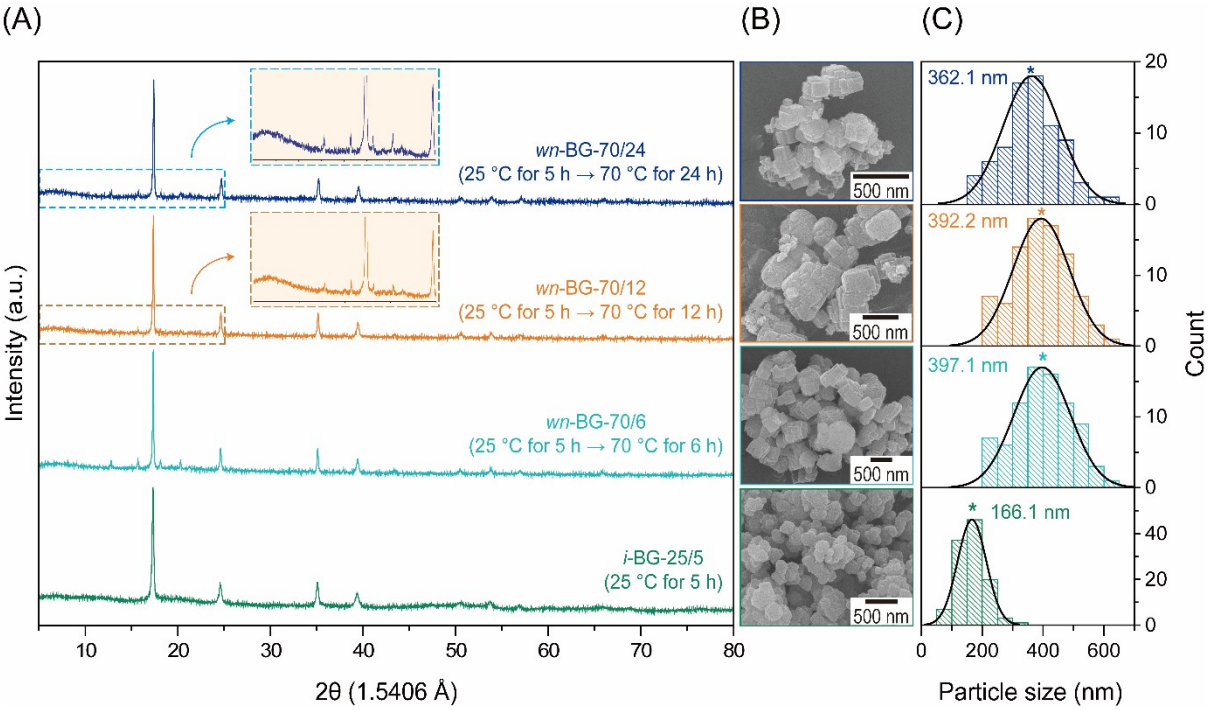

Fig. S3. (A) XRD patterns and (B) SEM images of a series of *wn*-BG-70/t samples. (C) Particle size distribution curves of *wn*-BG-70/t samples.

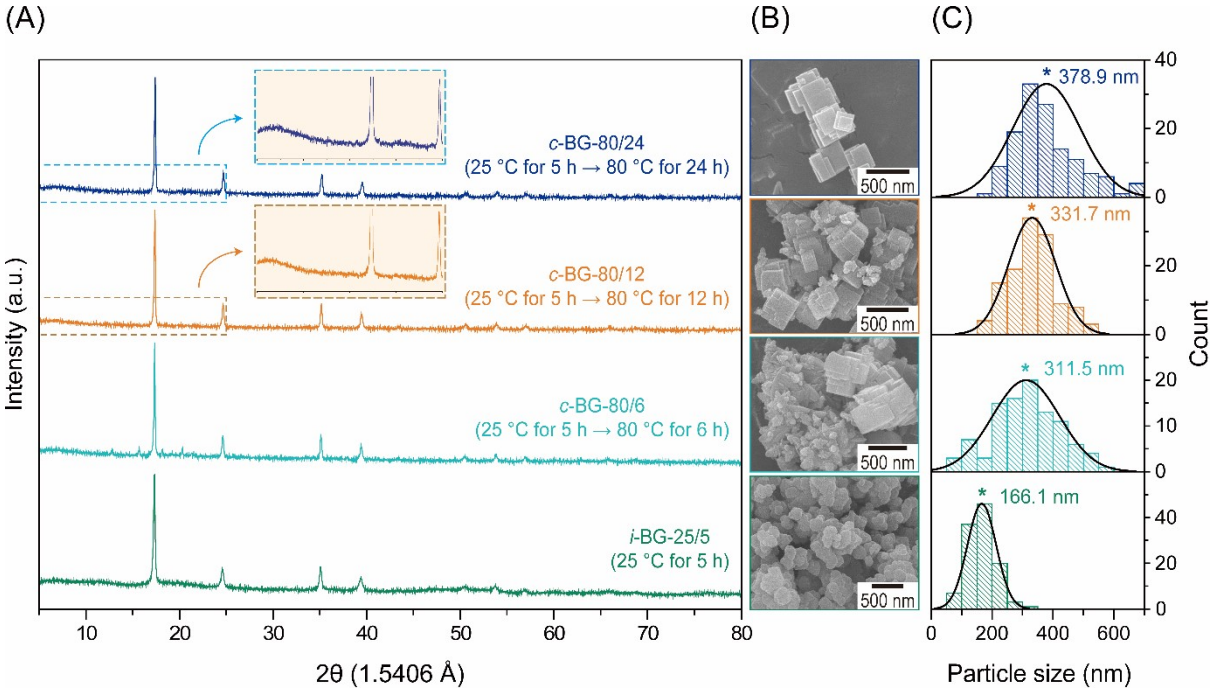

Fig. S4. (A) XRD patterns and (B) SEM images of a series of *c*-BG-80/t samples. (C) Particle size distribution curves of *c*-BG-80/t samples.

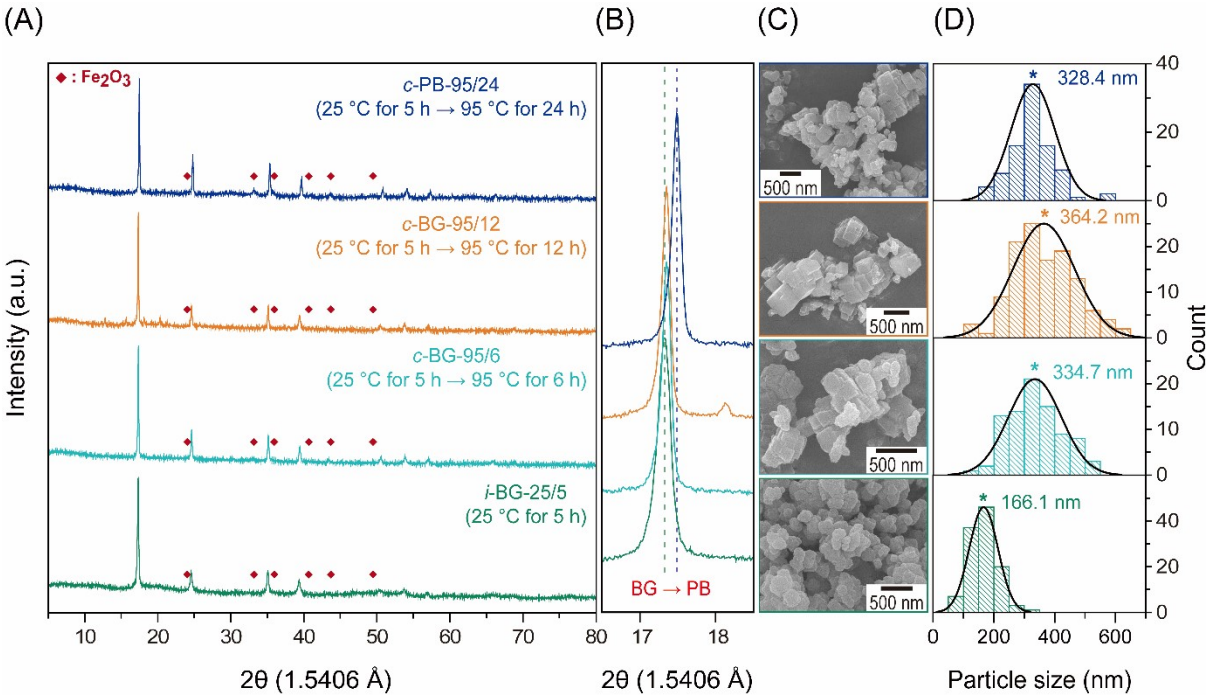

Fig. S5. (A) XRD patterns of a series of *c*-PB-95/t samples and (B) magnified XRD patterns in the 2θ range of 16.5°–18.5°. (C) SEM images and (D) particle size distribution curves of a series of *c*-PB-95/t samples.

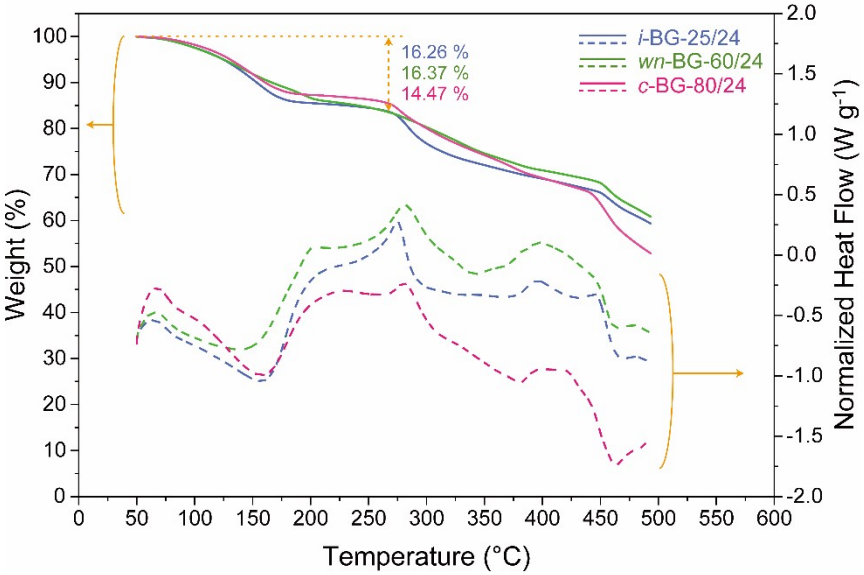

Fig. S6. TGA/DSC profiles of *i*-BG-25/24, *wn*-BG-60/24, and *c*-BG-80/24.

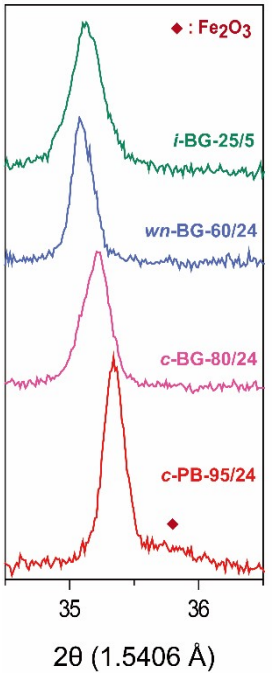

Fig. S7. Magnified XRD profiles of Fig. 2A in the 2θ range of 34.5°–36.5° to display (400) reflections.

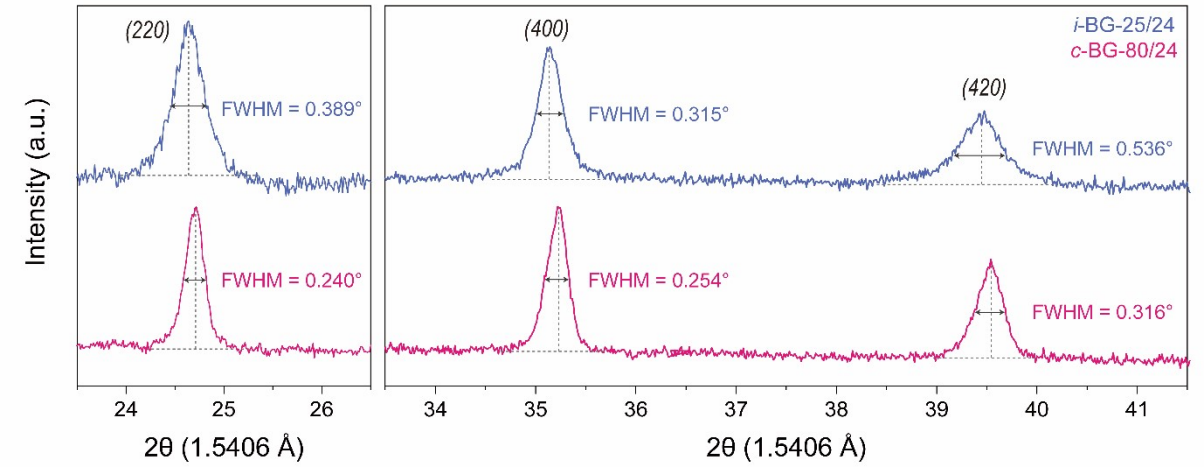

Fig. S8. Comparison of XRD patterns between *i*-BG-25/24 and *c*-BG-80/24 in the 2θ range of 23.5°–26.5° and 33.5°–41.5°, respectively.

i-BG-25/24 exhibited a larger full-width-at-half-maximum (FWHM) value of (400) peak (0.315°) compared with *c*-BG-80/24 (0.254°), indicating the less crystallinity and more flexible framework of *i*-BG-25/24. The initial high capacity originating from the structural flexibility of *i*-BG-25/24 caused increasing stress on the host framework, leading to capacity decay within only a few initial cycles.

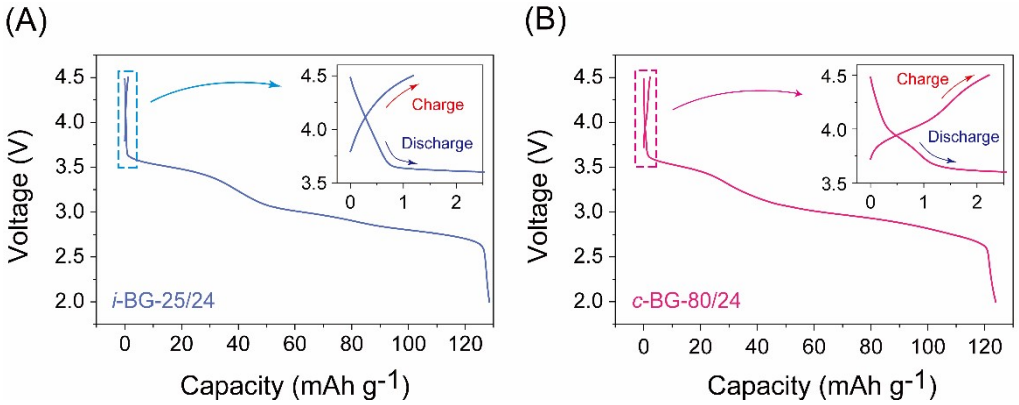

Fig. S9. Galvanostatic curves in the first cycle at a current density of 10 mA g^{-1}. (A) *i*-BG-25/24. (B) *c*-BG-80/24.

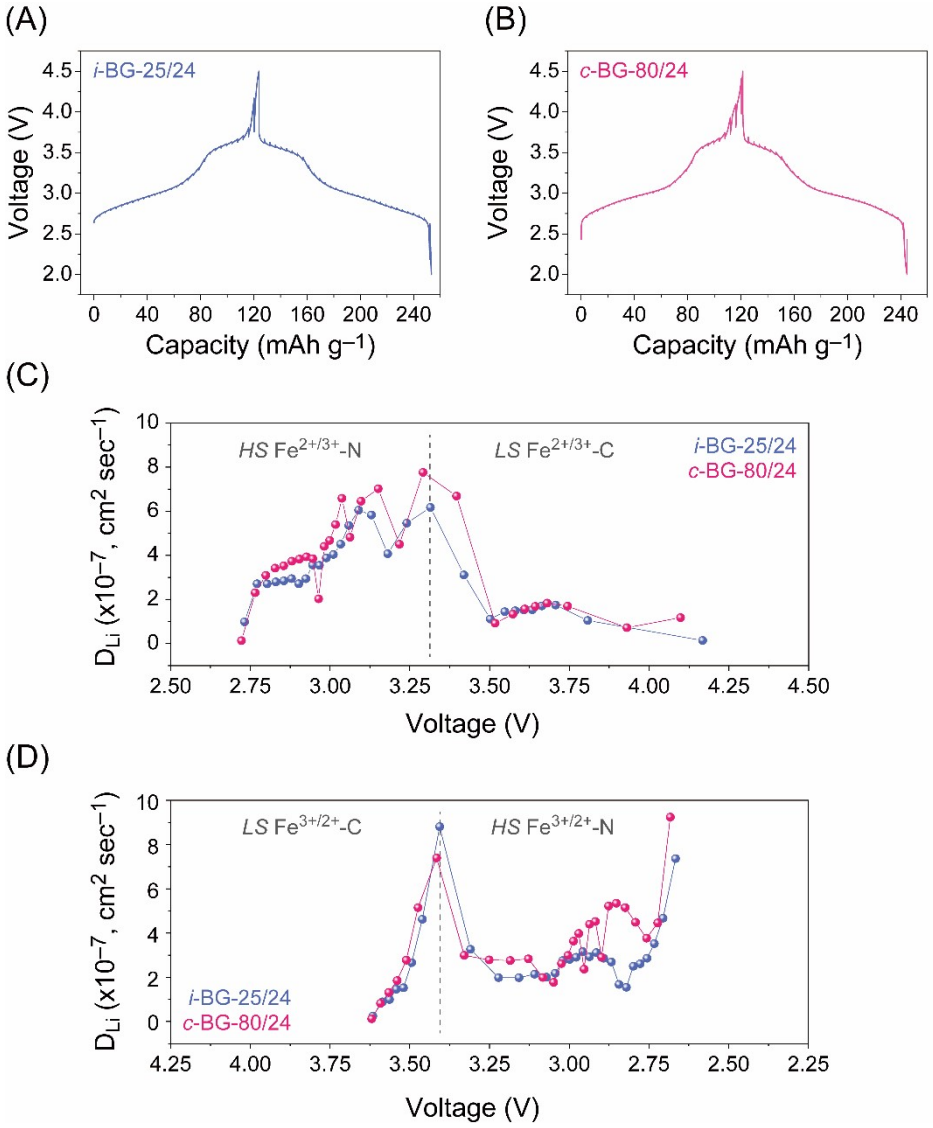

Fig. S10. (A–B) GITT curves and (C–D) calculated D_{Li} during the charge/discharge process.

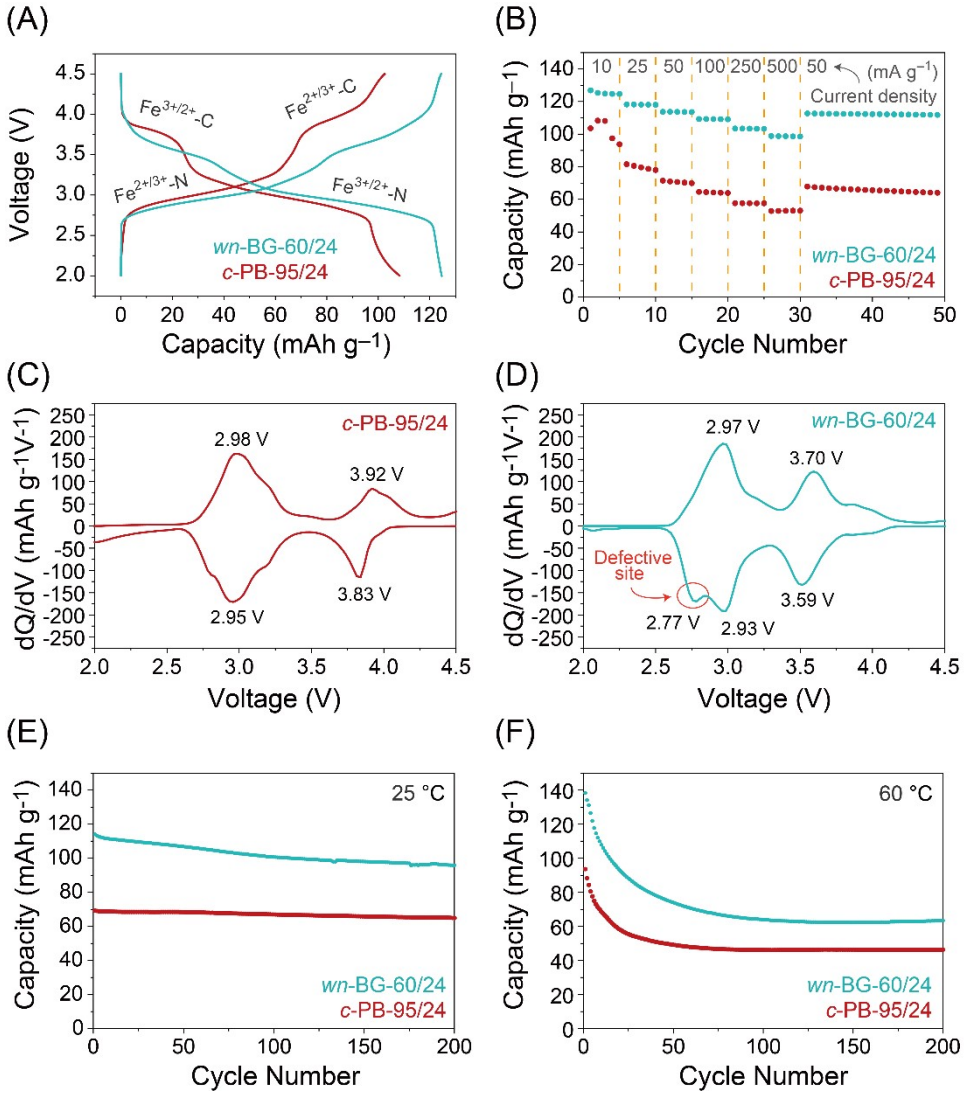

Fig. S11. Electrochemical evaluation of *wn*-BG-60/24 and *c*-PB-95/24. (A) Galvanostatic charge/discharge curves at a current density of 10 mA g^{-1}. (B) Rate capability measured at current densities of 10, 25, 50, 100, 250, and 500 mA g^{-1}. (C and D) Differential capacity (dQ/dV) *versus* voltage plots for *c*-PB-95/24 and *wn*-BG-60/24. (E and F) Cycling performance (E) at 25 °C and (F) 60 °C with a current density of 100 mA g^{-1}.

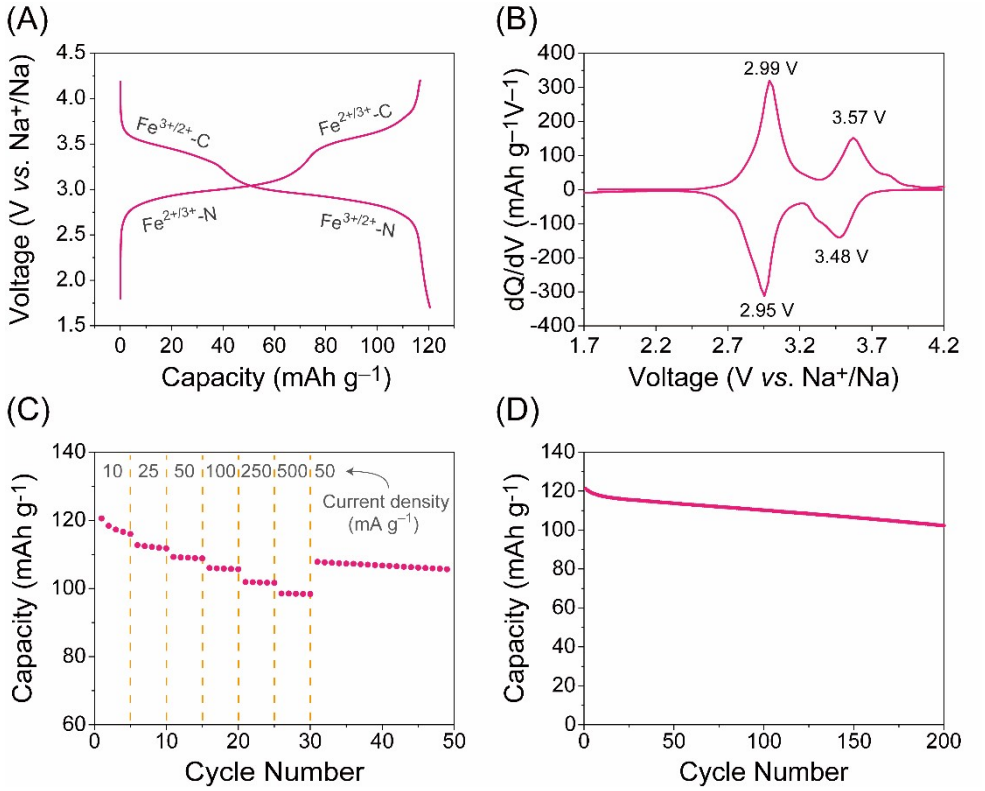

Fig. S12. Electrochemical evaluations of *c*-BG-80/24 in the SIB cell. (A) Galvanostatic charge/discharge curves at a current density of 10 mA g^{-1}. (B) Differential capacity (dQ/dV) *versus* voltage plot. (C) Rate capability measured at current densities of 10, 25, 50, 100, 250, and 500 mA g^{-1}. (D) Cycling performance at 25 °C.

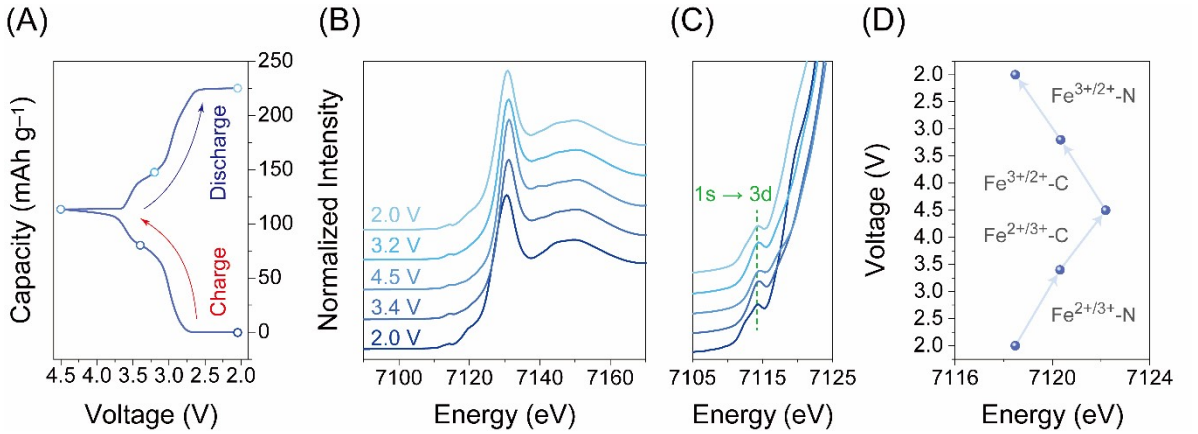

Fig. S13. XAFS characterizations for *i*-BG-25/24. (A) Typical galvanostatic charge/discharge curves of *i*-BG-25/24. (B) Normalized XANES spectra achieved at the Fe K-edge for *i*-BG-25/24 samples with different charging states. (C) Magnified XANES profiles showing the pre-edge region. The vertical dotted line in green visualizes the pre-edge peak shift. (D) The edge energy profile of *i*-BG-25/24 as a function of cell voltage along with the corresponding redox couples.

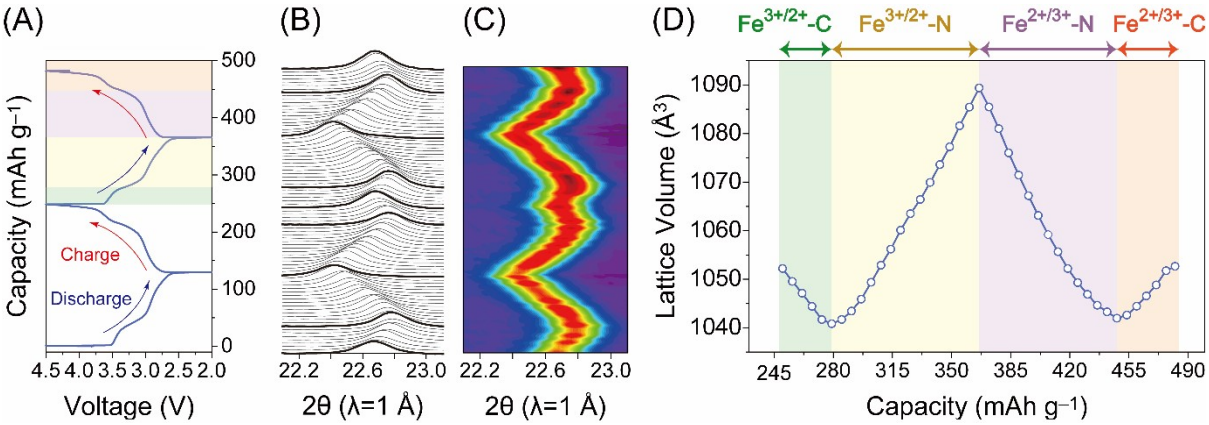

Fig. S14. *In situ* synchrotron XRD analyses of *i*-BG-25/24. (A) Galvanostatic charge/discharge profiles of *i*-BG-25/24 measured at 120 mA g^{-1} for two cycles during *in situ* XRD measurement. (B) XRD patterns in the 2θ range of 22.1°–23.1° to show the (400) reflection profile and (C) the corresponding contour plot. (D) Calculated lattice volume ($Å^3$) during the charge/discharge process in the second cycle.

Table S1. Elemental analysis results by ICP-OES.

	ICP-OES			**TGA/DSC**
	K (ppm)	Fe (ppm)	K/Fe ratio (mol/mol)	H_2O (*wt*%)[a]
i-BG-25/24	174.762	306698.933	0.000813881	16.26
wn-BG-60/24	6316.645	277718.199	0.032486921	16.37
c-BG-80/24	7134.223	360993.785	0.028227562	14.47

[a] Estimated by measuring the weight loss (%) from 50 °C to 266 °C.

Table S2. Comparison of the electrochemical performance of a series of BGs obtained in this study and that presented in previous reports.

	Shape	Operating voltage	Capacity (mAh g^{-1}) @ Current density (mA g^{-1})	Capacity retention (%) @ Cycle number (cycles)	Ref.
i-BG-25/24	Irregular	2.0–4.5 V *vs*. Li/Li^+	126.3 @ 10	77.6 @ 200	This study
wn-BG-60/24	Walnut	2.0–4.5 V *vs*. Li/Li^+	124.6 @ 10	80 @ 200	
c-BG-80/24	Cubic	2.0–4.5 V *vs*. Li/Li^+	124.3 @ 10	83.6 @ 200	
c-BG-80/24	Cubic	1.7–4.2 V *vs*. Na/Na^+	120.5 @ 10	84.4 @ 200	
c-PB-95/24	Cubic	2.0–4.5 V *vs*. Li/Li^+	108.3 @ 10	93.8 @ 200	
Na-MnHCF	Irregular	2.0 – 4.2 V *vs*. Na/Na^+	126 @ 30	60 @ 50	[10]
Na-FeHCF	Cubic	2.0 – 4.2 V *vs*. Na/Na^+	128 @ 30	76 @ 50	
Na-CoHCF	Irregular	2.0 – 4.2 V *vs*. Na/Na^+	100 @ 30	84 @ 50	
Na-NiHCF	Irregular	2.0 – 4.2 V *vs*. Na/Na^+	66 @ 30	Almost no capacity loss	
Co-PW	Cubic	2.0 – 4.1 V *vs*. Na/Na^+	150 @ 10	89.1 @ 200	[13]
KNiHCF	Irregular	2.0 – 4.5 V *vs*. K/K^+	62.8 @ 100	88.6 @ 100	[14]
Fe-PBA	Irregular	2.0 – 4.5 V *vs*. Li/Li^+	115 @ 10	50 @ 100	[21]

Co-PBA	Irregular	2.0 – 4.5 V *vs*. Li/Li^+	32 @ 10	96.7 @ 100	
Ni-PBA	Irregular	2.0 – 4.5 V *vs*. Li/Li^+	50 @ 10	96 @ 100	
Cu-PBA	Irregular	2.0 – 4.5 V *vs*. Li/Li^+	41 @ 10	112.8 @ 100	
NiFe-PBA	Irregular	2.0 – 4.1 V *vs*. Na/Na^+	73.8 @ 50	85.8 @ 1120	[23]
$FeFe(CN)_6$	Irregular	2.0 – 4.0 V *vs*. Na/Na^+	109 @ 60	87 @ 500	[30]
CoHCF-B (1M Na_2SO_4)	Cubic	0.0 – 1.0 V *vs*. SCE	110.8 @ 240	20.8 @ 2000	[33]
CoHCF-R (1M Na_2SO_4)	Cubic	0.0 – 1.0 V *vs*. SCE	115 @ 240	69.2 @ 2000	
Cu-PBA (1M $Li(NO_3)$)	N/A	0.0 – 1.2 V *vs*. SHE	51.36 @ 300	62 @ 50	[61]
Cu-PBA (1M $Na(NO_3)$)			56.80 @ 300	92 @ 50	
Cu-PBA (1M $K(NO_3)$)			55.15 @ 300	97 @ 50	
Cu-PBA (1M $Rb(NO_3)$)			41.44 @ 300	95.5 @ 50	
Cu-PBA (1M $Cs(NO_3)$)			28.30 @ 300	87 @ 50	